Fitoterapia 158 (2022) 105144

Contents lists available at ScienceDirect

Fitoterapia

journal homepage: www.elsevier.com/locate/fitote

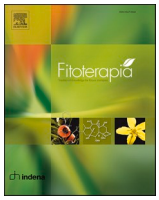

α-Pyrones with glucose uptake-stimulatory activity from the twigs of *Cryptocarya wrayi*

Xiao-Na Wang [a,#], Xiao-Dong Kuang [b,#], Yong Wang [a], Peng Sun [c], Xiao-Ru He [d], Yi-An Peng [a], Lu-Hong Liu [a], Jin-Long Gu [a], Li-She Gan [e], Xiao-Ning Wang [f], Ji-Cheng Shu [d,*], Zhi-Wang Zhou [a,d,**]

[a] School of Pharmacy, Nanchang University, Nanchang 330006, PR China
[b] Department of Pathology, School of Basic Medicine, Nanchang University, Nanchang 330006, PR China
[c] Key Laboratory of Tropical Plant Resources and Sustainable Use, Xishuangbanna Tropical Botanical Garden, Chinese Academy of Sciences, Menglun, Mengla, Yunnan 666303, PR China
[d] Key Laboratory of Modern Preparation of TCM, Ministry of Education, Jiangxi University of Chinese Medicine, Nanchang 330004, PR China
[e] School of Biotechnology and Health Sciences, Wuyi University, Jiangmen, Guangdong 529020, PR China
[f] Department of Natural Product Chemistry, Key Laboratory of Chemical Biology (Ministry of Education), School of Pharmaceutical Sciences, Shandong University, 44 West Wenhua Road, Jinan 250012, PR China

ARTICLE INFO

Keywords:
Cryptocarya wrayi
α-pyrone
Glucose uptake-stimulatory activity
ECD calculation

ABSTRACT

Five new α-pyrones, cryptowratones A-E (**1**–**5**), and five known congeners (**6**–**10**), together with four other known compounds **11**–**14** were isolated from the twigs of *Cryptocarya wrayi*. The structures of the new compounds were elucidated on the basis of extensive spectroscopic data analysis and ECD calculations. All α-pyrones except **6** were evaluated for their stimulatory effects on glucose uptake in vitro with CHO-K1/GLUT4 cells. The positive control insulin displayed an approximate 42 ± 0.14% promotion on glucose uptake at 25 μM, compared with the CHO-K1/GLUT4 group. Compounds **1a**/**2a**, **2**, **3**, and **10** showed a more significant stimulation of glucose uptake than insulin (25 μM) by 36 ± 0.08%, 27 ± 0.12%, 28 ± 0.12%, and 25 ± 0.12% at 1.5 μM, respectively. Immunofluorescence assays indicated the glucose uptake-stimulatory activity of α-pyrones might be correlated with increased GLUT4 translocation.

1. Introduction

The genus *Cryptocarya* (Lauraceae) comprising 200–250 species [1] is known as a rich resource of diverse secondary metabolites, such as α-pyrone derivatives [2,3], flavonoids [4–7], and alkaloids [8–10]. These components, particularly α-pyrones have drawn an increasing attention in recent years due to their multiple profound bioactivities, including NF-κB inhibitory [11], NO inhibitory [12], cytotoxic [13,14], antimalarial [15], and antitrypanosomal [16] activities as well as ability to stabilize the tumor suppressor Pdcd4 [14,17]. Moreover, the unique architectures of α-pyrones featuring interesting stereoisomerism also have stimulated efforts toward their total synthesis [18,19] in synthetic communities.

Diabetes is a serious, chronic metabolic disease characterized by hyperglycemia and it has been considered as a major threat to human health worldwide [20]. More than 463 million people were diabetic in 2019, and this number will soar to 700 million by 2045, according to the statistics presented by International Diabetes Federation [21]. Type-2 diabetes mellitus (T2DM) is the major type of diabetes owing to the relative inefficient use of insulin produced by the body. Glucose transporters are membrane proteins family comprising 13 members that responsible for glucose uptake in human body. Glucose transporter 4 (GLUT4) is a principal glucose transporter that is activated in response to insulin and facilitate the transport of glucose across the plasma membrane [22]. The impaired translocation or decreased expression of GLUT4 is considered one of the major pathological features of T2DM

* Corresponding authors at: Key Laboratory of Modern Preparation of TCM, Ministry of Education, Jiangxi University of Chinese Medicine, Nanchang 330004, PR China.
* Corresponding authors at: School of Pharmacy, Nanchang University, Nanchang 330006, PR China.
E-mail addresses: shujc210@jxutcm.edu.cn (J.-C. Shu), zhouzw@ncu.edu.cn (Z.-W. Zhou).
# These authors contributed equally to this work

https://doi.org/10.1016/j.fitote.2022.105144
Received 7 January 2022; Received in revised form 6 February 2022; Accepted 6 February 2022
Available online 8 February 2022
0367-326X/

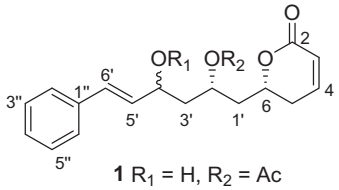

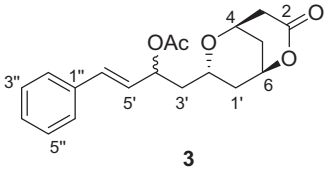

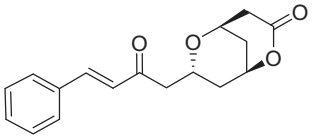

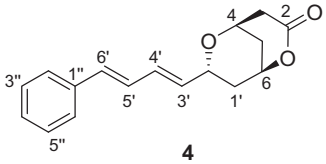

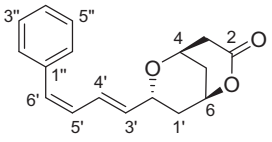

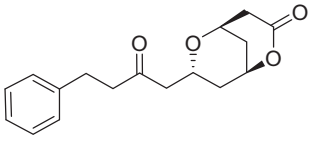

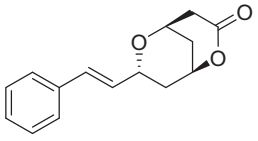

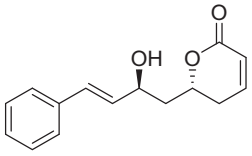

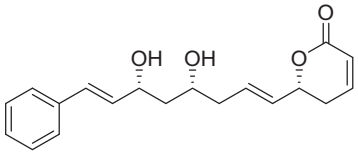

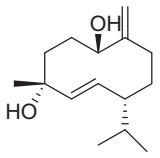

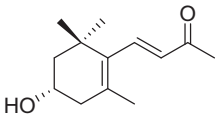

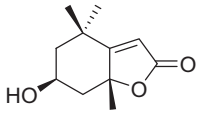

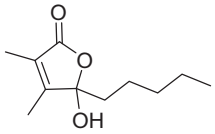

[23]. Therefore, inducing the translocation and expression of GLUT4 is a promising strategy for anti-T2DM drug discovery. In an effort for discovering natural metabolites with hypoglycemic activity from Lauraceous plants, we have studied the twig extracts of *Cryptocarya wrayi* and isolated five new α-pyrone derivatives, cryptowratones A-E (**1**–**5**), five known analogues, cryptoyunone E (**6**) [24], pulchrinervialactone B (**7**) [25], 7-styryl-2, 6-dioxabicyclo[3,3,1]nonan-3-one (**8**) [26,27], deacetyl cryptocaryalactone (**9**) [26], and cryptomoscatone E1 (**10**) [28], together with four other known compounds nephthediol (**11**) [29], 3*S*)-3-hydroxy-β-ionone (**12**) [30], (−)-loliolide (**13**) [31], and 4-hydroxy-2, 3-dimethylnon-2-en-4-olide (**14**) [32]. Herein, the identification of new compounds as well as the glucose uptake activities in CHO-K1/GLUT4 cells of α-pyrones were reported.

2. Experimental

2.1. General experimental procedures

Optical rotations were measured on an Anton Paar MCP-200 polarimeter. UV spectra were obtained on a Shimadzu UV-2550 Spectrophotometer. ECD spectra were measured on a JASCO J-815 spectropolarimeter in MeOH. The 1D- and 2D- NMR were recorded on a Bruker AVANCE 400 NMR spectrometer with tetramethylsilane (TMS) as an internal reference. All HRESI-MS spectra were analyzed on a Waters UPLC-QTOF mass spectrometer equipped with ESI source (Waters, Milford, MA, USA). Silica gel (300–400 mesh, Qingdao Marine Chemical Plant, Qingdao, P. R. China), C_{18} reversed-phase silica gel (150–200 mesh, Merck), MCI gel (CHP20P, 75–150 μM, Mitsubishi Chemical Industries Ltd., Japan), and Sephadex LH-20 gel (75–150 μM, GE Healthcare, USA) were used for column chromatography. Precoated silica gel GF_{254} plates (Qingdao Marine Chemical Plant) were used for TLC. Semi-preparative HPLC was performed on an Agilent 1200 system equipped with a VWD G1314B detector and a YMC-Pack ODS-A column (250 × 10 mm, 5 μm). For the glucose uptake bioassay, cell culture materials and the glucose assay kit were obtained from Jiancheng (Nanjing, Jiangsu, China). 6, 4′-Diamidino-2-phenylindole (DAPI) was from KeyGEN BioTECH Corp., Ltd. (Nanjing, Jiangsu, China). Anti-GLUT4 was from Proteintech (Chicago, IL, USA). Goat anti-rabbit antibody IgG cy3 were from ABclonal Technology (Wuhan, Hubei, China). Other chemicals were of analytical grade.

2.2. Plant material

The twigs of *Cryptocarya wrayi* (6.0 kg) were collected from the Xishuangbanna Tropical Botanical Garden, Yunnan Province, China, in June 2018 and authenticated by Professor You-Kai Xu of Xishuangbanna Tropical Botanical Garden, Chinese Academy of Sciences. A voucher specimen (CW201806) has been deposited in the School of Pharmaceutical Sciences, Nanchang University.

2.3. Extraction and isolation

The air-dried and pulverized twigs of *C. wrayi* (6.0 kg) were extracted with 95% EtOH three times at room temperature. The crude extract (285.0 g) was then suspended in water and subsequently extracted with petroleum ether, EtOAc, and *n*-BuOH, successively. The EtOAc extract (38.5 g) was fractionated by MCI gel column chromatography (CC) using a MeOH/H_2O gradient system (30: 70 → 100: 0 , *v*/v) to afford seven

Table 1
^{1}H and ^{13}C NMR Spectroscopic Data for Compounds **1** and **2.**

No.	**1**[a]		**2**[a]	
	δ_H	δ_C	δ_H	δ_C
2		164.1		164.0
3	6.01, dd, 10.0, 2.4	121.5	6.03, dt, 9.6, 2.0	121.4
4	6.86, ddd, 10.0, 6.0, 2.4	145.0	6.89, dt, 9.6, 4.4	145.3
5	a 2.31, ddt, 18.4, 11.6, 2.4 b 2.47, ddd, 18.4, 6.0, 4.0	29.4	2.40, m, 2H	29.6
6	4.52, m	75.2	4.67, m	76.8[b]
1′	a 2.00, m b 2.23, m	39.7	a 1.84, m b 1.88, m	42.4
2′	5.25, m	68.3	3.98, m	66.7
3′	a 1.91, m b 2.05, m	41.7	2.03, m, 2H	42.2
4′	4.44, q, 6.4	70.1	5.60, q, 6.8	73.0
5′	6.21, dd, 16.0, 6.4	131.4	6.16, dd, 16.0, 7.2	126.9
6′	6.58, d, 16.0	130.7	6.68, d, 16.0	133.4
1′′		136.5		136.1
2′′	7.37, d, 7.2	126.6	7.38, t, 7.2	126.8
3′′	7.32, t, 7.2	128.8	7.32, t, 7.2	128.8
4′′	7.24, t, 7.2	128.0	7.26, d, 7.2	128.3
5′′	7.32, t, 7.2	128.8	7.32, t, 7.2	128.8
6′′	7.37, d, 7.2	126.6	7.38, t, 7.2	126.8
-OAc	2.03, s	171.2 21.4	2.08, s	170.5 21.6

[a] Measured at 400 MHz in $CDCl_3$.
[b] Overlapped

Table 2
^{1}H and ^{13}C NMR spectroscopic data for Compounds **3**–**5.**

No.	**3**[a]		**4**[b]		**5**[b]	
	δ_H	δ_C	δ_H	δ_C	δ_H	δ_C
2		172.9		169.8		169.8
3α	2.87, dd, 19.2, 5.2	36.7	2.83, dd, 19.2, 5.6	36.6	2.80, dd, 19.2, 5.2	36.6
3β	2.65, d, 19.2		2.96, d, 19.2		2.94, d, 19.2	
4	4.32, m	67.3	4.45, m	66.2	4.41, m	66.1
5α	2.00, m	30.2	2.07, m	29.6	2.05, m	29.6
5β	2.00, m		1.96, m		1.93, m	
6	4.89, overlapped	75.0	4.94, m	73.0	4.92, m	73.0
1'α	1.69, ddd, 16.0, 12.0, 2.0	37.9	1.73, ddd, 16.0, 11.6, 2.0	37.2	1.70, ddd, 16.4, 11.6, 2.0	37.2
1'β	1.98, m		2.15, m		2.09, m	
2′	3.80, m	64.2	4.39, m	66.6	4.35, m	66.7
3'a	1.82, ddd, 13.6, 7.6, 3.6	41.2	5.75, dd, 15.2, 6.0	131.9	5.78, dd, 15.2, 6.4	134.2
3'b	1.99, m					
4′	5.59, q, 7.2	73.8	6.43, dd, 15.2, 10.4	132.2	6.79, dd, 15.2, 11.6	128.2
5′	6.16, dd, 16.0, 8.0	127.9	6.74, dd, 15.6, 10.4	127.9	6.21, t, 11.6	129.1
6′	6.66, d, 16.0	134.7	6.57, d, 15.6	133.8	6.49, d, 11.6	131.5
1′′		137.6		137.1		137.2
2′′	7.42, d, 7.2	127.7	7.39, d, 7.6	126.6	7.37, d, 7.2	128.5
3′′	7.32, t, 7.2	129.7	7.31, t, 7.6	128.8	7.29, t, 7.2	129.0
4′′	7.25, t, 7.2	129.1	7.23, t, 7.6	127.9	7.26, t, 7.2	127.4
5′′	7.32, t, 7.2	129.7	7.31, t, 7.6	128.8	7.29, t, 7.2	129.0
6′′	7.42, d, 7.2	127.7	7.39, d, 7.6	126.6	7.37, d, 7.2	128.5
-OAc	2.04, s	172.1 21.2				

[a] Measured at 400 MHz in CD_3OD.
[b] Measured at 400 MHz in $CDCl_3$.

fractions, Fr.1 − Fr.7. Fr.7 (3.5 g) was separated over Sephadex LH-20 (EtOH) to yield four subfractions, Fr.7A − Fr.7D. Fr·7C (476.8 mg) was subjected to CC on silica gel (petroleum ether/acetone 8: 1 → 2: 1 , v/v) to give four subfractions, Fr·$7C_1$ − Fr·$7C_4$, and fractions Fr·$7C_2$ (104.8 mg) was then purified by semi-preparative HPLC (CH_3CN/H_2O, 40: 60, 3.0 mL/min) to afford **5** (2.0 mg, t_R = 40.2 min). Fr·$7C_3$ (62.0 mg) was purified by semi-preparative HPLC (CH_3CN/H_2O, 37: 63, 3.0 mL/min) to afford **4** (0.7 mg, t_R = 59.5 min). Fr.5 (3.47 g) was subjected to CC with Sephadex LH-20 (EtOH) to give three subfractions, Fr.5A − Fr·5C. Fr·5C (206.0 mg) was purified by CC on silica gel (petroleum ether/acetone 3: 1 → 0: 1 , v/v) to afford three subfractions, Fr·$5C_1$ − Fr.$5C_3$. Fr·$5C_1$ (10.0 mg) was then purified by semi-preparative HPLC (CH_3CN/H_2O, 40: 60, 3.0 mL/min) to afford **9** (0.8 mg, t_R = 22.5 min). Fr·$5C_2$ (23.6 mg) was purified by semi-preparative HPLC (CH_3CN/H_2O, 30: 70, 3.0 mL/min) to afford **6** (0.6 mg, t_R = 28.5 min) and **7** (1.7 mg, t_R = 33.7 min). Fr.5A (170.3 mg) was separated by CC on silica gel (petroleum ether/acetone 3: 1 → 0: 1 , v/v) to afford three subfractions, Fr.$5A_1$ − Fr.$5A_3$. Fr.$5A_2$ (21.6 mg) was then purified by semi-preparative HPLC (CH_3CN/H_2O, 38: 62, 3.0 mL/min) to afford **1** (2.2 mg, t_R = 21.5 min) and **2** (2.7 mg, t_R = 26.2 min). Fr.$5A_1$ (14.9 mg) was purified by semi-preparative HPLC (CH_3CN/H_2O, 40: 60, 3.0 mL/min) to afford **3** (1.3 mg, t_R = 32.0 min). Fr.$5A_3$ (14.9 mg) was then purified by semi-preparative HPLC (CH_3CN/H_2O, 30: 70, 3.0 mL/min) to afford **8** (0.8 mg, t_R = 37.3 min). Fr.4 (2.8 g) was subjected to CC with Sephadex LH-20 (EtOH) to give two subfractions, Fr.4A and Fr·4B. Fr.4A (687.9 mg) was purified by CC on silica gel (petroleum ether/acetone 4: 1 → 1.5: 1 v/v) to afford two subfractions, Fr.$4A_1$ and Fr.$4A_2$. Fr.$4A_1$ (77.7 mg) was purified by semi-preparative HPLC (CH_3CN/H_2O, 35: 65, 3.0 mL/min) to afford **11** (2.6 mg, t_R = 31.9 min). Fr·4B (1.0 g) was subjected to CC on silica gel (petroleum ether/acetone 8: 1 → 0: 1 v/v) to afford eight subfractions, Fr·$4B_1$ − Fr.$4B_8$. Fr·$4B_1$ (20.7 mg) was purified by semi-preparative HPLC (CH_3CN/H_2O, 40: 60, 3.0 mL/min) to afford **14** (1.1 mg, t_R = 24.7 min). Fr·$4B_3$ (24.4 mg) was purified by semi-preparative HPLC (CH_3CN/H_2O, 28: 72, 3.0 mL/min) to afford **12** (2.1 mg, t_R = 23.5 min) and **13** (0.3 mg, t_R = 12.1 min). Fr·$4B_6$ (20.0 mg) was purified by semi-preparative HPLC (CH_3CN/H_2O, 30: 70, 3.0 mL/min) to afford **10** (1.8 mg, t_R = 29.2 min).

*Cryptowratone A (**1**):* yellowish gum; [α]25 D + 39.6 (c 0.22, MeOH); UV λ_{max} (log ε) 252 (2.99) nm; ECD (c 2.0 × 10^{-4} gmL^{-1}, MeOH) λ ($\Delta\varepsilon$) 203 (+8.58), 236 (+1.20), 254 (+2.43) nm; ^{1}H NMR (400 MHz) and ^{13}C NMR (100 MHz) data, see Table 1; (+)-HRESI-MS *m/z* 353.1363 $[M + Na]^+$ (calcd for $C_{19}H_{22}O_5Na$, 353.1365), (−)-HRESI-MS *m/z* 329.1393 $[M-H]^-$ (calcd for $C_{19}H_{21}O_5$, 329.1389).

*Cryptowratone B (**2**):* yellowish gum; [α]25 D + 38.1 (c 0.20, MeOH); UV λ_{max} (log ε) 292 (2.64) nm; ECD (c 2.0 × 10^{-4} gmL^{-1}, MeOH) λ ($\Delta\varepsilon$) 203 (+7.41), 236 (+1.02), 255 (+2.03) nm; ^{1}H NMR (400 MHz) and ^{13}C NMR (100 MHz) data, see Table 1; (+)-HRESI-MS *m/z* 353.1363 $[M + Na]^+$ (calcd for $C_{19}H_{22}O_5Na$, 353.1365), (−)-HRESI-MS *m/z* 329.1393 $[M-H]^-$ (calcd for $C_{19}H_{21}O_5$, 329.1389).

*Cryptowratone C (**3**):* yellowish gum; [α]25 D + 22.5 (c 0.04, MeOH); UV λ_{max} (log ε) 251 (3.97) nm; ECD (c 2.0 × 10^{-4} gmL^{-1}, MeOH) λ ($\Delta\varepsilon$) 204 (+2.26), 223 (−1.39), 253 (+1.44) nm; ^{1}H NMR (400 MHz) and ^{13}C NMR (100 MHz) data, see Table 2; (+)-HRESI-MS *m/z* 683.2817 $[2 M + Na]^+$ (calcd for $C_{38}H_{44}O_{10}Na$, 683.2832).

*Cryptowratone D (**4**):* yellowish gum; [α]25 D -5.0 (c 0.04, MeOH); UV λ_{max} (log ε) 285 (3.46) nm; ECD (c 2.0 × 10^{-4} gmL^{-1}, MeOH) λ ($\Delta\varepsilon$) 200 (−1.26), 207 (−2.39), 283 (+0.31) nm; ^{1}H NMR (400 MHz) and ^{13}C NMR (100 MHz) data, see Table 2; (+)-HRESI-MS *m/z* 293.1163 $[M + Na]^+$ (calcd for $C_{17}H_{18}O_3Na$, 293.1154).

*Cryptowratone E (**5**):* yellowish gum; [α]25 D -6.4 (c 0.14, MeOH); UV λ_{max} (log ε) 242 (3.26) nm; ECD (c 2.0 × 10^{-4} gmL^{-1}, MeOH) λ ($\Delta\varepsilon$) 200 (−2.46), 206 (−4.26), 243 (+1.69) nm; ^{1}H NMR (400 MHz) and ^{13}C NMR (100 MHz) data, see Table 2; (+)-HRESI-MS *m/z* 271.1326 $[M + H]^+$ (calcd for $C_{17}H_{19}O_3$, 271.1334).

2.4. Acetylation of *1* and *2*

Each compound (1.0 mg) was treated with Ac_2O (2.0 mL) and dried pyridine (100 μL) overnight at room temperature. The reaction mixture was extracted with CH_2Cl_2 (5 mL× 3) and then purified using semi-

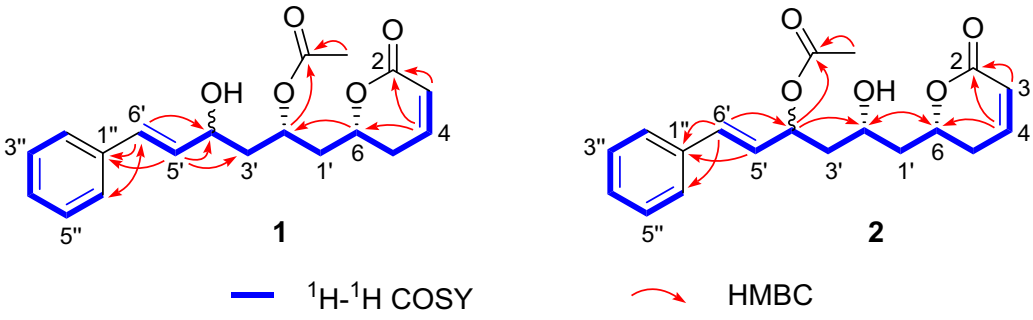

Fig. 1. ^{1}H—^{1}H COSY and key HMBC correlations of **1** and **2**.

preparative HPLC with $CH_3CN - H_2O$ (42: 58 *v*/v).

*O-Acetyl derivatives of **1** and **2** (**1a**/**2a**)*: [α]25 D + 16.67 (c 0.06, MeOH); ^{1}H NMR (400 MHz, $CDCl_3$) δ_H 7.37 (2H, d, J = 7.2 Hz, H-2″/H-6″), 7.32 (2H, t, J = 7.2 Hz, H-3″/H-5″), 7.26 (1H, H-4″, overlapped), 6.86 (1H, ddd, J = 9.6, 6.0, 2.4 Hz, H-4), 6.61 (1H, d, J = 16.0 Hz, H-6′), 6.10 (1H, dd, J = 16.0, 7.2 Hz, H-5′), 6.01 (1H, dd, J = 9.6, 2.8 Hz, H-3), 5.49 (1H, q, J = 6.8 Hz, H-4′), 5.12 (1H, m, H-2′), 4.50 (1H, m, H-6), 2.45 (1H, ddd, J = 18.4, 5.2, 4.4 Hz, H-5b), 2.30 (1H, ddt, J = 18.4, 11.6, 2.4 Hz, H-5a), 2.09 (3H, s, 4′-OAc), 2.06 (3H, s, 2′-OAc); (+)-HRESI-MS *m/z* 395.1462 $[M + Na]^+$ (calcd for $C_{21}H_{24}O_6Na$, 395.1465), *m/z* 767.3038 $[2 M + Na]^+$ (calcd for $C_{42}H_{48}O_{12}Na$, 767.3038).

2.5. ECD calculation

The absolute configurations of compounds **3**–**5** was determined by quantum chemical TDDFT calculations of their theoretical ECD spectra. Firstly, conformational analysis of all compounds was carried out via Monte Carlo searching using molecular mechanism with MMFF94 force field in the Spartan 08 program [33] in the relative energy window of 0–2 Kcal/mol. The conformers were then reoptimized using DFT at the B3LYP/6-31G(d) level in vacuum in the Gaussian 09 program [34]. The B3LYP/6-31G(d) harmonic vibrational frequencies were further calculated to confirm their stability. The energies, oscillator strengths, and rotational strengths of the first 40 electronic excitations were calculated using the TDDFT methodology at the B3LYP/6–311++G(2d,2p) level in vacuum. The ECD spectra were simulated by the overlapping Gaussian function (σ = 0.3 eV) [35], in which velocity rotatory strengths of the first 40 exited states for compounds **3**–**5** was adopted. To get the conformationally averaged ECD spectra, the simulated spectra of the lowest energy conformers were averaged according to the Boltzmann distribution theory and their relative Gibbs free energy (ΔG).

2.6. Cell culture

CHO-K1 cell line was purchased from the Institute of Biochemistry and Cell Biology, Chinese Academy of Sciences. The CHO-K1/GLUT4 cells were generated by GLUT4-overexpressing lentivirus infection at the *Genechem* Co., Ltd., Shanghai, China. All cells were cultured in F-12 K medium with 2 mM L-glutamine supplemented with 5% fetal bovine serum and maintained in a humidified incubator at 37 °C with 5% CO_2.

2.7. Glucose uptake assay

CHO-K1 and CHO-K1/GLUT4 cells were seeded at a density of 3 × 10^3 cells/well in Costar 48-well plates and incubated overnight to adhere. The cells were then treated with insulin (150 μg/mL, as a positive control) or test samples at three concentrations within the dose of 50, 5, and 0.5 μg/mL, respectively. After incubation for 48 h, cells were fixed with 4% formaldehyde in PBS for 15 min at room temperature. The wells were washed three times with 100 μL of PBS. The glucose levels were determined using a glucose assay kit.

2.8. Cell viability assay

The cell viability was evaluated using the CCK8 method. CHO-K1 cells in 96-well culture plates were treated with various concentrations of the test compounds. After incubation with 100 μL culture medium for the indicated time, 10 μL CCK8 reagent was added to each well and incubated at 37 °C for 2 h. The absorbance at 450 nm was measured using a WD-2102B microplate reader (Liuyi Biotechnology Co., Ltd., Beijing, China).

2.9. Immunofluorescence

CHO-K1/GLUT4 cells were seeded at a density of 3 × 10^4 cells/well in Costar 48-well plates and incubated overnight to adhere. Cells were then treated with different concentrations of test compounds. After 48 h of treatment, cells were fixed with 4% formaldehyde in PBS for 15 min, washed three times with PBS, and then quenched with 0.5%Triton X-100 in PBS for 20 min. Cells were blocked with 5% BSA in PBS for 30 min at 37 °C and incubated with anti-GLUT4 antibody C-myc (1: 200 dilution in 3% BSA in PBS) overnight at 4 °C. After washing with PBS, cells were incubated with secondary antibody IgG cy3 (1: 200 dilution in 3% BSA in PBS) for 45 min at 37 °C. Cells were washed with PBS and mounted with Mounting Medium with DAPI. Images were obtained using a confocal laser microscope (FV1000, Olympus, Japan).

2.10. Statistical analysis

Statistical analyses employed Dunnett's *t*-test using the GraphPad Prism 8.2 software (San Diego, CA, USA). A p value less than 0.05 was deemed to indicate statistical significance.

3. Results and discussion

Cryptowratone A (**1**) was obtained as a yellow gum. Its molecular formula was determined to be $C_{19}H_{22}O_5$ based on the (+)-HRESI-MS at *m/z* 353.1363 $[M + Na]^+$ (calcd for $C_{19}H_{22}O_5Na$, 353.1365) and (−)-HRESI-MS at *m/z* 329.1393 $[M-H]^-$ (calcd for $C_{19}H_{21}O_5$, 329.1389), requiring 9 degrees of unsaturation (DOU). The ^{1}H NMR spectrum of **1** (Table 1) displayed signals attributable to a α-pyrone derivative [2,12], including a mono-substituted benzene [δ_H 7.37 (2H, d, J = 7.2 Hz, H-2″ and H-6″), 7.32 (2H, t, J = 7.2 Hz, H-3″ and H-5″), and 7.24 (1H, t, J = 7.2 Hz, H-4″)], one *cis*- double bond [δ_H 6.01 (1H, dd, J = 10.0, 2.4 Hz, H-3) and 6.86 (1H, ddd, J = 10.0, 6.0, 2.4 Hz, H-4)], one *trans*- double bond [δ_H 6.21 (1H, dd, J = 16.0, 6.4 Hz, H-5′) and 6.58 (1H, d, J = 16.0 Hz, H-6′)], three oxymethines [δ_H 4.52 (1H, m, H-6), 5.25 (1H, m, H-2′), and 4.44 (1H, q, J = 6.4 Hz, H-4′)], an acetoxy group [δ_H 2.03 (3H, s)], and six aliphatic protons in the upfield region. The ^{13}C NMR spectrum (Table 1) combining with HSQC data indicated that **1** contains 19 carbons, which comprise two ester carbonyls (δ_C 171.2 and 164.1), ten aromatic/olefinic carbons, three oxymethines (δ_C 75.2, 68.3, and 70.1), three methylenes, and one acetoxy methyl carbon (δ_C 21.4).

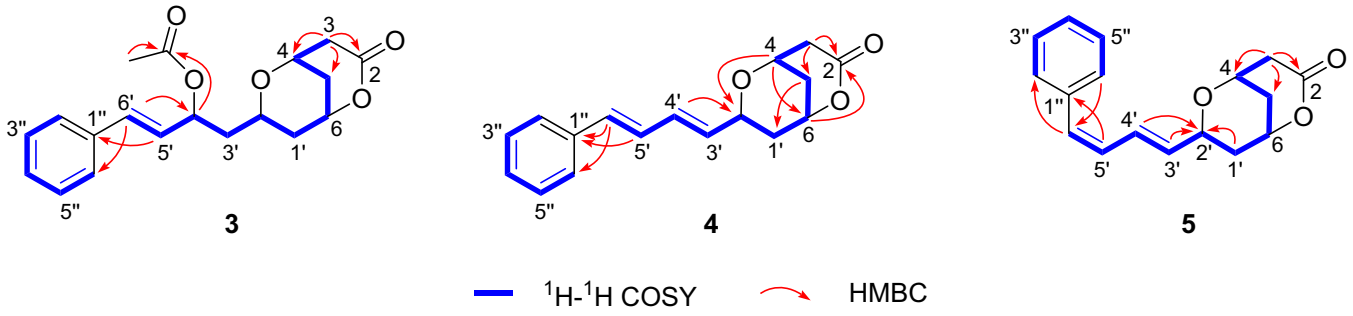

Fig. 2. ^{1}H—^{1}H COSY and key HMBC correlations of **3**–**5**.

Comprehensive analysis of the ^{1}H—^{1}H COSY and HMBC spectra allowed the establishment of the planar structure of **1**. The ^{1}H—^{1}H COSY correlations of H-4/H-3 and H_2–5; H-6/H_2–5 and H_2–1′; H-2′/H_2–1′ and H_2–3′; H-4′/H_2–3′ and H-5′; H-5′/H-6′; H-4″/H-3″ and H-5″; H-2″(6″)/H-3″(5″) deduced the bold fragments as shown in Fig. 1. The acetoxy group was located at C-2′ by the HMBC correlations from H-2′ (δ_H 5.25) and CH_3 (δ_H 2.03) to one ester carbonyl (δ_C 171.2). Another ester carbonyl (δ_C 164.1) was assigned to C-2 by the HMBC correlations of H-3 and H-4/C-2. The monosubstituted benzene was connected to C-6′ by the HMBC correlations of H-5′ and H-6′/C-1″, H-6′/C-2″ and C-6″, H-2″ and H-6″/C-6′. Taking into account of one remaining DOU unassigned for **1**, the presence of one characteristic α, β-unsaturated δ-lactone moiety was determined by the chemical shift of C-2 (δ_C 164.1) and C-6 (δ_C 75.2). The characteristic separate chemical shifts and splitting patterns of the C-5 protons at δ_H 2.31 and 2.47 suggested a 6, 2′-*syn* relative configuration [36,37]. The absolute configuration at C-6 was determined to be *R* based on the positive Cotton effect [12,17] at 254 nm in the ECD spectrum of **1**. Due to the scarcity of **1**, the absolute configuration at C-4′ was failed to be determined by using the Mosher's method.

Cryptowratone B (**2**) was also purified as a yellow gum. Its molecular formula was assigned as $C_{19}H_{22}O_5$ based on the (+)-HRESI-MS at *m/z* 353.1363 $[M + Na]^+$ (calcd for $C_{19}H_{22}O_5Na$, 353.1365) and (−)-HRESI-MS *m/z* 329.1393 $[M-H]^-$ (calcd for $C_{19}H_{21}O_5$, 329.1389). Its 1D-NMR data (Table 1) was highly related with those of **1** and suggested it was probably the 4'-OAc isomer of the latter. Two spin systems were also deduced as drawn with bold lines in Fig. 1 from the ^{1}H—^{1}H COSY spectrum of **2**. The attachment of 4'-OAc was corroborated by the HMBC correlations (Fig. 1) from H-4′ (δ_H 5.60) and CH_3 (δ_H 2.08) to one ester carbonyl (δ_C 170.5). Similarly, the position of another ester carbonyl (δ_C 164.0, C-2) and the monosubstituted benzene were determined by the HMBC correlations of H-5′ and H-6′/C-1″, H-6′/C-2″ and C-6″, H-3 and H-4/C-2. The α, β-unsaturated δ-lactone was also retained according to the chemical shift of C-2 (δ_C 164.0) and C-6 (δ_C 76.8). Therefore, the gross structure of **2** was then completely constructed. The absolute configuration at C-6 was determined to be *R* based on the positive Cotton effect [12,17] at 255 nm in its ECD spectrum. To establish the absolute configurations of C-2′ in **2**, the hydroxy groups in **1** and **2** were acetylated using Ac_2O in pyridine. The acetylation product **2a** exhibited the distinctive chemical shifts and splitting patterns of the C-5 protons separately at 2.45 and 2.30 for a 6, 2′-*syn* relative configuration [36,37]. Furthermore, the HPLC retention time, ^{1}H NMR data, and specific rotation of **2a** were identical to those of **1a**. Thus, the absolute configuration at C-2′ was established as *R*.

Cryptowratone C (**3**), a yellow gum, was assigned the molecular formula $C_{19}H_{22}O_5$ by ^{13}C NMR and HRESIMS data (m/z 683.2817 [2 M + Na]$^+$, calcd for $C_{38}H_{44}O_{10}Na$, 683.2832), requiring 9 DOUs. Its 1D-NMR spectra (Table 2) were very similar to that of **2**. However, the signals for the *cis*-olefin at C-3 and C-4 were absent, while oxymethine and germinal aliphatic signals were observed at δ_H 4.32 (1H, m), 2.87 (1H, dd, 19.2, 5.2 Hz), and 2.65 (1H, d, 19.2 Hz), respectively. These observations indicated **3** was probably the corresponding bicyclic tetrahydro-α-pyrone derivative of **2**. Comprehensive 2D-NMR spectra, including HSQC, ^{1}H—^{1}H COSY and HMBC, allowed the establishment of the planar structure as shown in Fig. 2. Similarly, the ^{1}H—^{1}H COSY correlations of H-4/H_2–3 and H_2–5; H-6/H_2–5 and H_2–1′; H-2′/H_2–1′ and H_2–3′; H-4′/H_2–3′ and H-5′; H-5′/H-6′; H-4″/H-3″ and H-5″; and H-2″(6″)/H-3″(5″) established the two relative segments of **3**. The acetoxy group was located at C-4′ by the HMBC correlations of H-4′ (δ_H 5.59) and CH_3 (δ_H 2.04) to one ester carbonyl (δ_C 172.1). The location of the monosubstituted benzene and another ester carbonyl (δ_C 172.9, C-2) were determined by the HMBC correlations of H-5′/C-1″, H-6′/C-2″ and C-6″, and H_2–3/C-2. The bicyclic δ-lactone fragment was deduced from the chemical shift of C-2 (δ_C 172.9), C-4 (δ_C 67.3), and C-6 (δ_C 75.0) to meet 9 DOUs. The NOESY correlation (Fig. 3) of H-2′/H-3β indicated the bicyclic pyrone **3** adopted the thermodynamically favored chair-like conformation, which was more readily produced from a 6, 2′-*syn* precursor [3]. The orientation of substituents at C-6 in **3** biogenetically must be the same with that of **2** and established an *S* configuration for C-

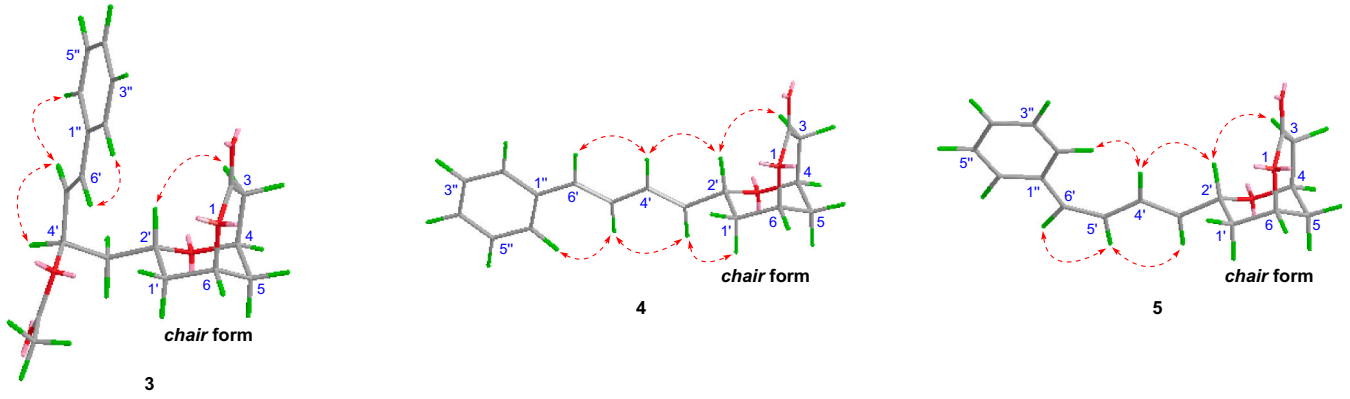

Fig. 3. Key NOESY correlations of compounds **3**–**5**.

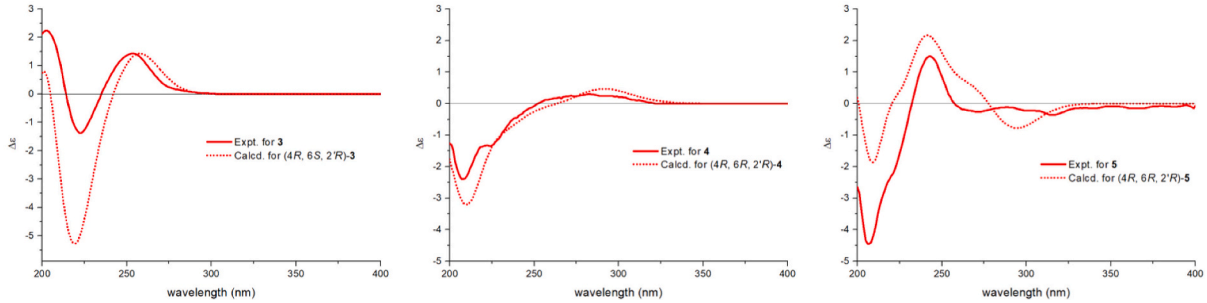

Fig. 4. Experimental and calculated ECD spectra of compounds **3**–**5**.

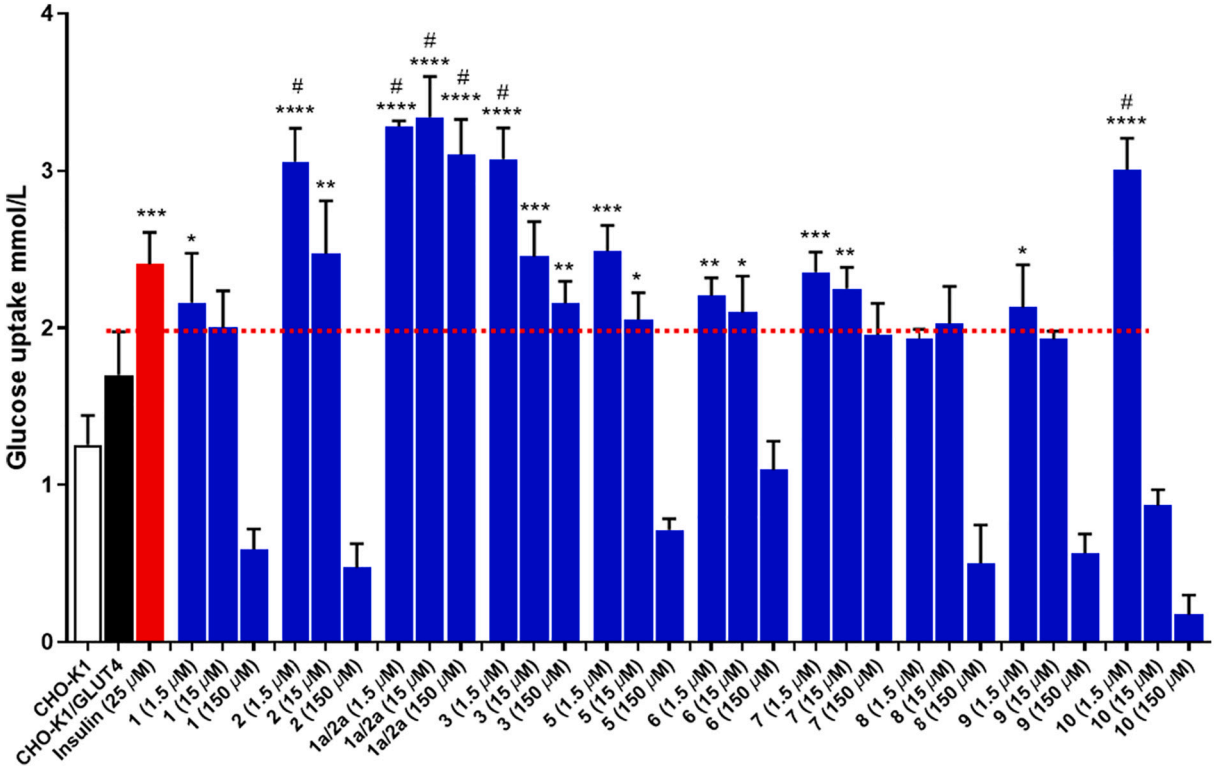

Fig. 5. Stimulation effects of α-pyrones on glucose uptake in CHO-K1/GLUT4 cells. The results were calculated as the mean ± SEM ($n = 6$); each experiment was performed in triplicate; $^{*}p < 0.05$, $^{**}p < 0.01$, $^{***}p < 0.001$, and $^{****}p < 0.0001$, compared to the CHO-K1/GLUT4 group; $^{\#}p < 0.001$, compared to the insulin group.

6 due to a change in group priorities. The preference for the formation of a less-strained *cis* fused bicyclic system dictates the generation of a 4*R*-configured center [3,15]. Thus, the 4*R**, 6*S**, 2′*R**-configuration for **3** was tentatively assigned. To verify the above deduction, a quantum chemical calculation of the theoretical ECD spectrum was employed by using the TDDFT method. The experimental ECD spectrum of **3** matched well with the calculated ECD curve of 4*R*, 6*S*, 2′*R*-**3** (Fig. 4). Hence, the absolute configuration of **3** was determined to be 4*R*, 6*S*, 2′*R*.

Cryptowratone D (**4**) and Cryptowratone E (**5**) were purified as a pair of isomers with the molecular formula $C_{17}H_{18}O_3$, as determined by (+)-HRESIMS spectra. Besides signals for a mono-substituted benzene and the bicyclic lactone fragment, the ^{1}H NMR spectra (Table 2) also displayed signals for a *trans/trans* conjugated diene [δ_H 5.75 (1H, dd, J = 15.2, 6.0 Hz, H-3′), 6.43 (1H, dd, J = 15.2, 10.4 Hz, H-4′), 6.74 (1H, dd, J = 15.6, 10.4 Hz, H-5′), and 6.57 (1H, d, J = 15.6 Hz, H-6′)] system in **4** and/or a *trans/cis* conjugated diene [δ_H 5.78 (1H, dd, J = 15.2, 6.4 Hz, H-3′), 6.79 (1H, dd, J = 15.2, 11.6 Hz, H-4′), 6.21 (1H, t, J = 11.6 Hz, H-5′), and 6.49 (1H, d, J = 11.6 Hz, H-6′)] motif in **5**, respectively. Their planar structures were then deduced as shown in Fig. 2 by extensive 2D-NMR spectra including HSQC, ^{1}H—^{1}H COSY and HMBC. Furthermore, the *E/E* conformation of the $\Delta^{3',4'}/\Delta^{5',6'}$ conjugated double bonds in **4** was identified by NOESY correlations of H-3′/H-5′ and H-4′/H-6′, while the NOESY correlations of H-3′/H-5′ and H-5′/H-6′ in **5** established its $\Delta^{3',4'}/\Delta^{5',6'}$ diene moiety as the *E/Z* conformation. The 4*R**, 6*R**, 2′*R**-configuration for **4** and **5** was tentatively determined similarly according to the key NOESY correlation of H-2′/H-3β (Fig. 3) and biogenetical relationships. Finally, compounds **4** and **5** were also performed the quantum chemical calculations of their theoretical ECD spectra (Fig. 4) and allowed the assignment of 4*R*, 6*R*, 2′*R*- configuration for **4** and **5**.

All α-pyrones except **6** were evaluated for their stimulatory effects on glucose uptake in vitro with CHO-K1/GLUT4 cells, a lentivirus-transduced CHO-K1 cell lines which can overexpress the GLUT4 protein. The positive control insulin displayed an approximate 42 ± 0.14% promotion on glucose uptake at 25 μM, comparing to the CHO-K1/GLUT4 group (Fig. 5). Most of the test compounds significantly improve the cell glucose absorption at the concentration of 1.5 μM and 15.0 μM. Compounds **1a**/**2a**, **2**, **3**, and **10** showed a remarkable stimulation of glucose uptake by 36 ± 0.08%, 27 ± 0.12%, 28% ± 0.12%, and

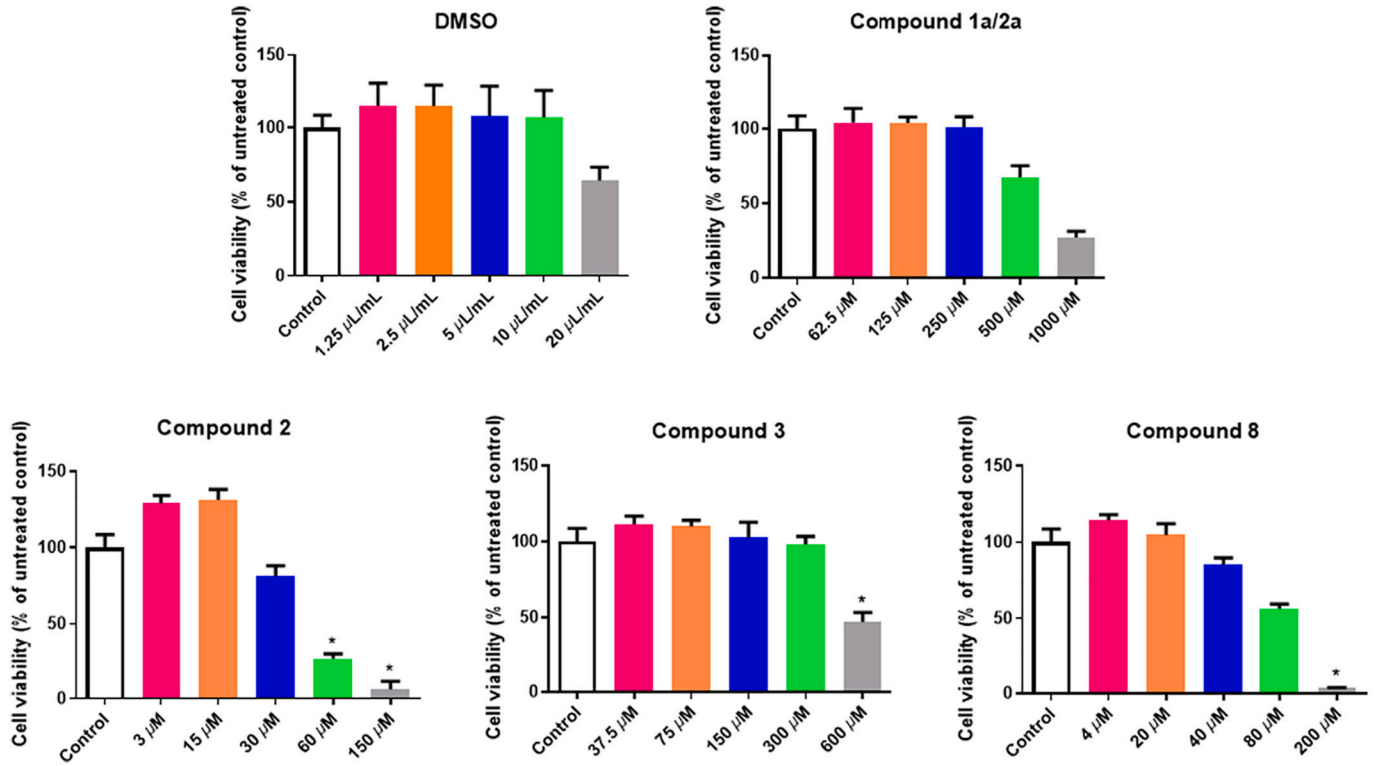

Fig. 6. Proliferation effect of selected α-pyrones on CHO-K1 cell lines; The results were calculated as the mean ± SD ($n = 5$); each experiment was performed in triplicate; *$p < 0.05$, compared to the control group.

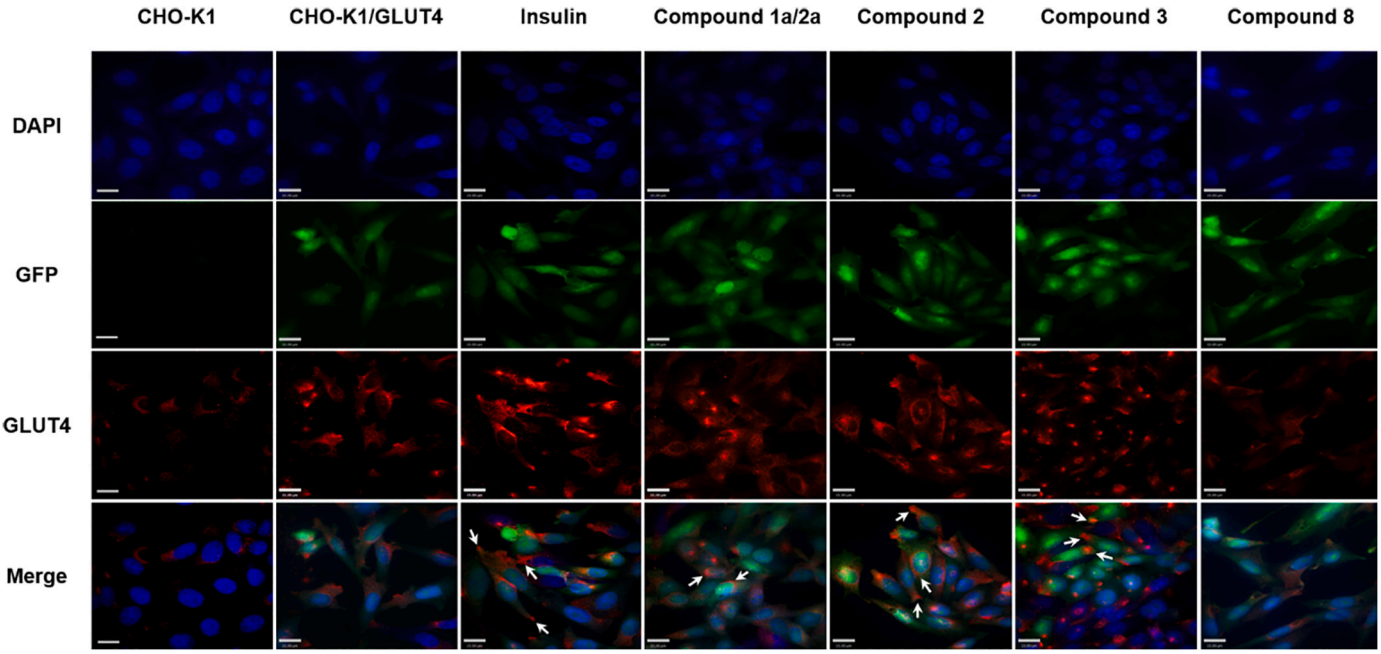

Fig. 7. Confocal microscopy images of GLUT4 expression in CHO-K1/GLUT4 cells. CHO-K1/GLUT4 cells were treated with insulin (25 μM) or 1.5 μM of α-pyrones (**1a**/**2a**, **2**, **3**, and **8**) for 48 h. Fluorescence intensities were measured using anti-GLUT4 and secondary antibody IgG cy3. Scale bar = 15 μm.

25 ± 0.12% at 1.5 μM, respectively, compared with insulin (25 μM). All α-pyrones show a downward trend on glucose absorption from 15.0 μM to 150 μM, indicated they was cytotoxic toward the CHO-K1 cell lines at high concentrations. Some α-pyrones such as **1**, **2**, **4**, **5**, and **8**–**10** significantly damaged the cells and decreased their metabolic ability at the concentration of 150 μM.

Compounds **1a**/**2a**, **2**, **3**, and **8** were then selected to detect their proliferative effects on the wild CHO-K1 cell by CCK8 method. The cytotoxic effect of each compound is shown in Fig. 6, and their IC_{50} were calculated as: **1a**/**2a** (524.3 ± 0.26 μM), **2** (34.2 ± 0.05 μM) and **3** (602.2 ± 0.33 μM), and **8** (125.6 ± 0.14 μM). This result indicated **1a**/**2a** and **3** might be good hit compounds for further development.

Glucose uptake in insulin-sensitive cells is mediated mainly by GLUT4, which is translocated from GLUT4 vesicles in the cytoplasm to

the plasma membrane. To determine whether the ability of α-pyrones to enhance glucose uptake is correlated with increased GLUT4 translocation, immunofluorescence was performed. After immunofluorescence operation, the samples were imaged by laser confocal imaging, and the results are shown in Fig. 7. The red signal of secondary antibody showed that the GLUT4 protein overexpressed in CHO-K1/GLUT4 cells. After treatment with insulin or compounds **1a**/**2a**, **2** and **3**, GLUT4 displayed a circular distribution or local aggregation close to the cell membranes, suggesting that these α-pyrones might increase GLUT4 translocation.

4. Conclusion

In this study, eleven α-pyrones including one synthetic congener were reported from the twigs of *Cryptocarya wrayi* and their glucose uptake-stimulatory activity were evaluated. Among them, **1a**/**2a** and **3** exhibited potent enhancement on glucose uptake of the CHO-K1/GLUT4 cells without cytotoxity. Moreover, immunofluorescence assays showed the glucose uptake-stimulatory activity of α-pyrones might be correlated with increased GLUT4 translocation. These results suggested that α-pyrones from *Cryptocarya* species could be a potential source of compounds with antidiabetic properties.

Credit author statement

Xiao-Na Wang: Compound isolation and structural elucidation.
Xiao-Dong Kuang: Bioactivities screen.
Yong Wang: Compound isolation.
Peng Sun: ECD calculation.
Xiao-Ru He: HR-ESIMS measurement.
Yi-An Peng: Cell culture.
Lu-Hong Liu: Sample concentration.
Jin-Long Gu: Plant extraction.
Li-She Gan: Data processing and analysis on ECD calculation.
Xiao-Ning Wang: UV and ECD measurement.
Ji-Cheng Shu: Data curation and formal analysis.
Zhi-Wang Zhou: Manuscript preparation and revision.

Declaration of Competing Interest

The authors declare no competing financial interest.

Acknowledgements

This research was supported by the National Natural Science Foundation of China (No. 21362023 and 22077111); the Natural Science Foundation of Jiangxi Province (20151BAB205083 and 20212ACB206006); the College Students' Innovative Entrepreneurial Training Plan Program (No. 202010403079); the Postgraduate Innovation Special Fund Project of Nanchang University (CX2019134); the Open Project of Key Laboratory of Modern Preparation of TCM, Ministry of Education, Jiangxi University of Chinese Medicine (No. zdsys-202104); and the '1050' Talents Program of Jiangxi University of Chinese Medicine (No. 5142001004). We thank Prof. You-Kai Xu of Xishuangbanna Tropical Botanical Garden, Chinese Academy of Sciences (CAS), for the identification of the plant material.

Appendix A. Supplementary data

Supplementary data to this article can be found online at https://doi.org/10.1016/j.fitote.2022.105144.

References

[1] X.W. Li, J. Li, H. van der Werff, Flora of China (Zhongguo Zhiwu Zhi), Science Press: Beijing, China 7 (2008) 247–254.
[2] F. Tsurumi, Y. Miura, M. Nakano, Y. Saito, S. Fukuyoshi, K. Miyake, D.J. Newman, B.R. O'Keefe, K.H. Lee, K. Nakagawa-Goto, Spiro[3.5]nonenyl meroterpenoid lactones, Cryptolaevilactones G-L, an ionone derivative, and total synthesis of Cryptolaevilactone M from *Cryptocarya laevigata*, J. Nat. Prod. 82 (2019) 2368–2378.
[3] F. Tsurumi, Y. Miura, Y. Saito, K. Miyake, T. Fujie, D.J. Newman, B.R. O'Keefe, K. H. Lee, K. Nakagawa-Goto, Secondary metabolites, monoterpene-polyketides containing a spiro[3.5]nonane from *Cryptocarya laevigata*, Org. Lett. 20 (2018) 2282–2286.
[4] Q. He, Y. Fan, Y. Liu, L. Rao, Y.X. You, Y. Su, Z. Zhou, Y.K. Xu, C.R. Zhang, Cryptoyunnanones A–H, complex flavanones from *Cryptocarya yunnanensis*, J. Nat. Prod. 84 (2021) 2209–2216.
[5] W. Huang, W.J. Zhang, Y.Q. Cheng, R. Jiang, W. Wei, C.J. Chen, G. Wang, R. H. Jiao, R.X. Tan, H.M. Ge, Cytotoxic and antimicrobial flavonoids from *Cryptocarya concinna*, Planta Med. 80 (2014) 925–930.
[6] Y. Ren, C. Yuan, Y. Qian, H.B. Chai, X. Chen, M. Goetz, A.D. Kinghorn, Constituents of an extract of *Cryptocarya rubra* housed in a repository with cytotoxic and glucose transport inhibitory effects, J. Nat. Prod. 77 (2014) 550–556.
[7] R. Feng, T. Wang, W. Wei, R.X. Tan, H.M. Ge, Cytotoxic constitutents from *Cryptocarya maclurei*, Phytochemistry 90 (2013) 147–153.
[8] W.N.N.W. Othman, Y. Sivasothy, S.Y. Liew, J. Mohamad, M.A. Nafiah, K. Ahmad, M. Litaudon, K. Awang, Alkaloids from *Cryptocarya densiflora* Blume (Lauraceae) and their cholinesterase inhibitory activity, Phytochem. Lett. 21 (2017) 230–236.
[9] W.N.N.W. Othman, S.Y. Liew, K.Y. Khaw, V. Murugaiyah, M. Litaudon, K. Awang, Cholinesterase inhibitory activity of isoquinoline alkaloids from three *Cryptocarya* species (Lauraceae), Bioorg. Med. Chem. 24 (2016) 4464–4469.
[10] Y. Suzuki, Y. Saito, M. Goto, D.J. Newman, B.R. O'Keefe, K.H. Lee, K. Nakagawa-Goto, (−)-Neocaryachine, an antiproliferative pavine alkaloid from *Cryptocarya laevigata*, induces DNA double-strand breaks, J. Nat. Prod. 80 (2017) 220–224.
[11] T.L. Meragelman, D.A. Scudiero, R.E. Davis, L.M. Staudt, T.G. McCloud, J. H. Cardellina II, R.H. Shoemaker, Inhibitors of the NF-κB activation pathway from *Cryptocarya rugulosa*, J. Nat. Prod. 72 (2009) 336–339.
[12] B.Y. Yang, L.Y. Kong, X.B. Wang, Y.M. Zhang, R.J. Li, M.H. Yang, J.G. Luo, Nitric oxide inhibitory activity and absolute configurations of arylalkenyl α, β-unsaturated δ/γ-lactones from *Cryptocarya concinna*, J. Nat. Prod. 79 (2016) 196–203.
[13] Y. Fan, Y. Liu, Y.X. You, L. Rao, Y. Su, Q. He, F. Hu, Y. Li, W. Wei, Y.K. Xu, B. Lin, C. R. Zhang, Cytotoxic arylalkenyl α, β-unsaturated δ-lactones from *Cryptocarya brachythyrsa*, Fitoterapia 136 (2019), 104167.
[14] M.F. Cuccarese, Y. Wang, P.J. Beuning, G.A. O'Doherty, Cryptocaryol structure-activity relationship study of cancer cell cytotoxicity and ability to stabilize Pdcd4, ACS Med. Chem. Lett. 5 (2014) 522–526.
[15] Y.X. Liu, H. Rakotondraibe, P.J. Brodie, J.D. Wiley, M.B. Cassera, J.S. Miller, F. Ratovoson, E. Rakotobe, V.E. Rasamison, D.G.I. Kingston, Antimalarial 5,6-dihydro-α-pyrones from *Cryptocarya rigidifolia*: related bicyclic tetrahydro-α-pyrones are artifacts, J. Nat. Prod. 78 (2015) 1330–1338.
[16] R.A. Davis, O. Demirkiran, M.L. Sykes, V.M. Avery, L. Suraweera, G.A. Fechner, R. J. Quinn, 7′, 8′-Dihydroobolactone, a typanocidal α-pyrone from the rainforest tree *Cryptocarya obovata*, Bioorg. Med. Chem. Lett. 20 (2010) 4057–4059.
[17] T. Grkovic, J.S. Blees, N.H. Colburn, T. Schmid, C.L. Thomas, C.J. Henrich, J. B. McMahon, K.R. Gustafson, Cryptocaryols A-H, α-pyrone-containing 1, 3-polyols from *Cryptocarya* sp. implicated in stabilizing the tumor suppressor pdcd4, J. Nat. Prod. 74 (2011) 1015–1020.
[18] X.L. Wang, W.K. Wang, H.J. Zheng, Y.P. Su, T. Jiang, Y.P. He, X.G. She, Efficient asymmetric total syntheses of cryptocarya triacetate, cryptocaryolone, and cryptocaryolone diacetate, Org. Lett. 11 (2009) 3136–3138.
[19] B. Melillo, A.B. Smith, A unified synthetic strategy to the cryptocarya family of natural products exploiting anion relay chemistry (ARC), Org. Lett. 15 (2013) 2282–2285.
[20] K.G. Alberti, P.Z. Zimmet, Definition, diagnosis and classification of diabetes mellitus and its complications. Part 1: diagnosis and classification of diabetes mellitus provisional report of a WHO consultation, Diabet. Med. 15 (1998) 539–553.
[21] S. Karuranga, B. Malanda, P. Saeedi, P. Salpea, *IDF Diabetes Atlas*, International Diabetes Federation 9 (2019) 6–7.
[22] R. Govers, Molecular mechanisms of GLUT4 regulation in adipocytes, Diabetes Metab. 40 (2014) 400–410.
[23] E.D. Abel, O. Peroni, J.K. Kim, Y.B. Kim, O. Boss, E. Hadro, T. Minnemann, G. I. Shulman, B.B. Kahn, Adipose-selective targeting of the GLUT4 gene impairs insulin action in muscle and liver, Nature 409 (2001) 729–733.
[24] Q. He, Y. Fan, Y. Liu, Y. X. You, L. Rao, Y. Su, Y. K. Xu, B. Lin, C. R. Zhang, Cytotoxic α-pyrone derivatives from *Cryptocarya yunnanensis*, Nat. Prod. Res. DOI: https://doi.org/10.1080/14786419.2020.1849205.
[25] L.D. Juliawaty, P.N. Ra'idah, S. Abdurrahman, E. Hermawati, A. Alni, M.I. Tan, H. Ishikawa, Y.M. Syah, 5, 6-Dihydro-α-pyrones from the leaves of *Cryptocarya pulchinervia* (Lauraceae), J. Nat. Med. 74 (2020) 584–590.
[26] S.E. Drewes, M.M. Horn, N.S. Ramesar, D. Ferreira, R.J.J. Nel, A. Hutchings, Absolute configurations of all four stereoisomers of cryptocaryalactone and deacetyl cryptocaryalactone, Phytochemistry 49 (1998) 1683–1687.
[27] S.E. Drewes, M.M. Horn, R.S. Shaw, α-Pyrones and their derivatives from two *Cryptocarya* species, Phytochemistry 40 (1995) 321–323.
[28] A.J. Cavalheiroa, M, Yoshida, 6-[ω-Arylalkenyl]-5, 6-dihydro-α-pyrones from *Cryptocarya moschata* (Lauraceae), Phytochemistry 53 (2000) 811–819.
[29] I. Kitagawa, Z. Cui, B.W. Son, M. Kobayashi, Y. Kyogoku, Marine natural products. XVII. Nephtheoxydiol, a new cytotoxic hydroperoxy-germacrane sesquiterpene,

and related sesquiterpenoids from an Okinawan soft coral of *Nephthea* sp. (Nephtheidae), Chem. Pharm. Bull. 35 (1987) 124–135.
[30] C. Pérez, J. Trujillo, L.N. Almonacid, J. Trujillo, E. Navarro, S.J. Alonso, Absolute structures of two new C_{13}-norisoprenoids from *Apollonias barbujana*, J. Nat. Prod. 59 (1996) 69–72.
[31] Y.H. Kuo, J.M. Lo, Y.F. Chan, Cytotoxic components from the leaves of *Schefflera taiwaniana*, J. Chin. Chem. Soc. 49 (2002) 427–431.
[32] L. Chen, S. Izumi, D.I. Ito, T. Iwaeda, R. Utsumi, T. Hirata, Secretion of allelochemicals from the cultured suspension cells of *Marchantia polymorpha*, Chem. Lett. 3 (1996) 205–206.
[33] Spartan 18; Wavefunction Inc.: Irvine, CA.
[34] M.J. Frisch, G.W. Trucks, H.B. Schlegel, G.E. Scuseria, M.A. Robb, J.R. Cheeseman, G. Scalmani, V. Barone, B. Mennucci, G.A. Petersson, H. Nakatsuji, M. Caricato, X. Li, H.P. Hratchian, A.F. Izmaylov, J. Bloino, G. Zheng, J.L. Sonnenberg, M. Hada, M. Ehara, K. Toyota, R. Fukuda, J. Hasegawa, M. Ishida, T. Nakajima, Y. Honda, O. Kitao, H. Nakai, T. Vreven, J.A. Montgomery Jr., J.E. Peralta, F. Ogliaro, M. Bearpark, J.J. Heyd, E. Brothers, K.N. Kudin, V.N. Staroverov, R. Kobayashi, J. Normand, K. Raghavachari, A. Rendell, J.C. Burant, S.S. Iyengar, J. Tomasi, M. Cossi, N. Rega, J.M. Millam, M. Klene, J.E. Knox, J.B. Cross, V. Bakken, C. Adamo, J. Jaramillo, R. Gomperts, R.E. Stratmann, O. Yazyev, A.J. Austin, R. Cammi, C. Pomelli, J.W. Ochterski, R.L. Martin, K. Morokuma, V.G. Zakrzewski, G.A. Voth, P. Salvador, J.J. Dannenberg, S. Dapprich, A.D. Daniels, Ö. Farkas, J. B. Foresman, J.V. Ortiz, J. Cioslowski, D.J. Fox, *Gaussian 09*, Revision A.1, Gaussian, Inc., Wallingford CT, 2009.
[35] P.J. Stephens, N. Harada, ECD cotton effect approximated by the Gaussian curve and other methods, Chirality 22 (2010) 229–233.
[36] T. Nakata, N. Hata, K. Nakashima, T. Oishi, Determination of the stereostructure of the δ-lactones of 5,7-dihydroxy-2,3-unsaturated acids by ^{1}H NMR spectroscopy, Chem. Pharm. Bull. 35 (1987) 4355–4358.
[37] T.J. Hunter, G.A. O'Doherty, An enantioselective synthesis of cryptocarya diacetate, Org. Lett. 3 (2001) 2777–2780.